1-1-2016

Molecular Parentage of Radical Species in the Comae of Comets

Benjamin Kyle Lewis

Molecular parentage of radical species in the comae of comets

By

Benjamin K. Lewis

A Thesis
Submitted to the Faculty of
Mississippi State University
in Partial Fulfillment of the Requirements
for the Degree of Master of Science
in Physics
in the Department of Physics and Astronomy

Mississippi State, Mississippi

May 2016

Molecular parentage of radical species in the comae of comets

By

Benjamin K. Lewis

Approved:

_____

Donna M. Pierce
(Major Professor)

_____

Angelle Tanner
(Committee Member)

_____

Chuji Wang
(Committee Member)
Choose an item.

_____

Henk F. Arnoldus
(Graduate Coordinator)

_____

Rick Travis
Interim Dean
College of Arts & Sciences

Name: Benjamin K. Lewis

Date of Degree: May 7, 2016

Institution: Mississippi State University

Major Field: Physics

Select Appropriate Title: Dr. Donna M. Pierce

Title of Study: Molecular parentage of radical species in the comae of comets

Pages in Study 31

Candidate for Degree of Master of Science

Understanding the chemical composition of comets is of great interest to the scientific community. In this work, an integral field unit (IFU) spectrograph is used to detect emissions of C_2, C_3, CH, CN, and NH_2. The azimuthal average profile (line integral of the column density as a function of radial distance from the center of the nucleus) is simulated by the Haser model. The Haser model simulates the outgassing and photo-dissociate of molecular species in the coma. In this work, the lifetime of the parent molecule in the photo-dissociation chain is set as a free parameter. The best fit parent lifetimes for observations of comets 4P/Faye, 10P/Tempel 2, and C/2009 P1 Garradd are obtained. The results are compared to parent lifetimes cited in other studies. HCN as a likely dominant parent for CN is eliminated. Constraints on likely parent molecules for C_3 and NH_2 are discussed.

TABLE OF CONTENTS

LIST OF TABLES

LIST OF FIGURES

CHAPTER I

INTRODUCTION

Comets (affectionately referred to as “Icy Travelers” by NASA) have four main components; a nucleus, coma, dust tail, and an ion tail. The composition is a mix of gases, ices, and rock. During early solar system, formation comets typically formed at distances from Neptune and beyond. Due to their small sizes and time spent in dynamical storage away from intense solar insolation, the chemical composition on the nucleus does not change significantly over fairly large timescales (relative to other solar system bodies); therefore, determining the relative abundances of the molecules (ices in particular) is of interest to the scientific community. It is also hypothesized by many that having a good understanding of cometary composition can provide constraints on solar system formation dynamics, particularly for modeling early solar system formation. For example, cometary composition could be strongly correlated with the chemical composition of the accretion disk in the regions where comets formed. (A’Hearn 2004). It is also hypothesized that during early solar system formation when comets collided with Earth, they could have delivered large quantities of water and organic compounds. One method for testing this hypothesis is comparing the Deuterium to Hydrogen ratio on Earth to the Deuterium to Hydrogen ratio on comets.

NASA, the European Space Agency, and other entities have launched a number of flyby missions to get a closer look at cometary composition and nucleus construction,

starting in 1978 with ISEE-3. Several of the more prominent missions include the Halley Armada, Deep Impact, and Stardust. The Halley Armada refers to a collection of five space probes which did fly-bys of 1P/Halley in 1986. The Halley Armada missions confirmed that 1P/Halley had a solid nucleus. Deep Impact successfully collided with the nucleus of 9P/Tempel 1 in 2005, which provided valuable insights on the dust/ice ratio in the nucleus composition and verified the existence of water ice in the nucleus. The Stardust spacecraft successfully returned to Earth in 2006 with dust samples from the coma of 81P/Wild 2. The samples returned included glycine, one of the 20 amino acids typically contained in proteins. A number of other interesting compounds were discovered, such as a number of different hydrocarbons. At this current date, the most exciting mission, and currently operational, is Rosetta, which entered orbit around 67P/Churyumov-Gerasimenko on August 6, 2014. This mission was also the first time we landed a spacecraft (Philae) on a comet. The Rosetta mission has and will continue to provide valuable insights about cometary chemistry (particularly about the nucleus).

In addition to *in situ* measurements, ground and space based observations can provide valuable insights about the comae of comets when their orbits bring them near the sun. When this happens, ices on the nucleus sublimate into gaseous compounds which then photo-dissociate into simpler radical molecules. These radicals can be detect through various spectroscopic methods.

The history of comet spectroscopy essentially began in 1864 with the detection of C_2 although it wasn't until identified as such until 1868 (Woodney 2000). By 1956, a number of radicals had been identified in cometary coma, including C_2, C_3, CH, CN, and

NH_2. The list of identifiable molecules from coma spectra continues to grow to this day (Feldman 2004).

Much of the current body of observations of radical species consists of narrowband photometry. The outgassing and photo-dissociation can be modeling through various computational models. The use of these models is necessary for the field of comet science because lab studies are often not applicable to comet conditions. In this work, we discuss observations obtain through an integral-field unit (IFU) spectrograph and use the Haser model in order to come to conclusions about cometary chemistry.

Data obtained from three comets were used in this study (4P/Faye, 10P/Tempel 2, and C/2009 P1 Garradd). Faye was discovered in 1843 and is a periodic Jupiter-family comet with an orbital period of 7.55 years. Faye's nucleus is estimated to be about 3.5 km in diameter. Tempel 2 was discovered in 1873 and is also a periodic Jupiter-family comet. It has an orbital period of 5.3 years and has an estimated nucleus diameter of 10.6 km. Garradd was first discovered in November 2009 and is a long-period comet from the Oort cloud with an estimated orbital period of 127,000 years. Garradd's orbit has high inclination with an orbital inclination of 106°, which is not unusual for an Oort Cloud comet.

CHAPTER II

OBSERVATIONS

Using The Mitchell Spectrograph

The data were obtained using an integral field unit (IFU) spectrograph on the 2.7 m Harlan J. Smith telescope at McDonald Observatory to conduct "full-coma" spectroscopic imaging. Images typically cover $\sim 2.5 \times 10^9$ km^2 of the target comet's coma. This instrument, the George and Cynthia Mitchell Spectrograph (formerly VIRUS-P) (Hill et al. 2008), is a high-efficiency, low- to moderate- resolution fiber-optic spectrograph. The 1.7 arcmin X 1.7 arcmin array contains 247 optical fibers, each with a diameter of 4.1 arcsec. The observations were obtained with a grating covering the passband from 3600-5800 Å with a resolving power of 850. Once the observations were made, the spectrum was processed via bias correction, flat fielding, wavelength and flux calibrations, and finally the sky spectrum is subtracted across the full passband (Cochran 2009). The dust continuum is also subtracted so that our observations reflect only gaseous emissions. Within this passband we are able to detect the emission of C_2, C_3, CH, CN, and NH_2. To obtain the path integral (along line of sight) of the column densities of the observed species for each optical fiber, standard g-factors (fluorescence efficiencies) are used. The result is a 2-D image of each species observed. A sample 2-D interpolated contour plot is demonstrated in Figure 1.

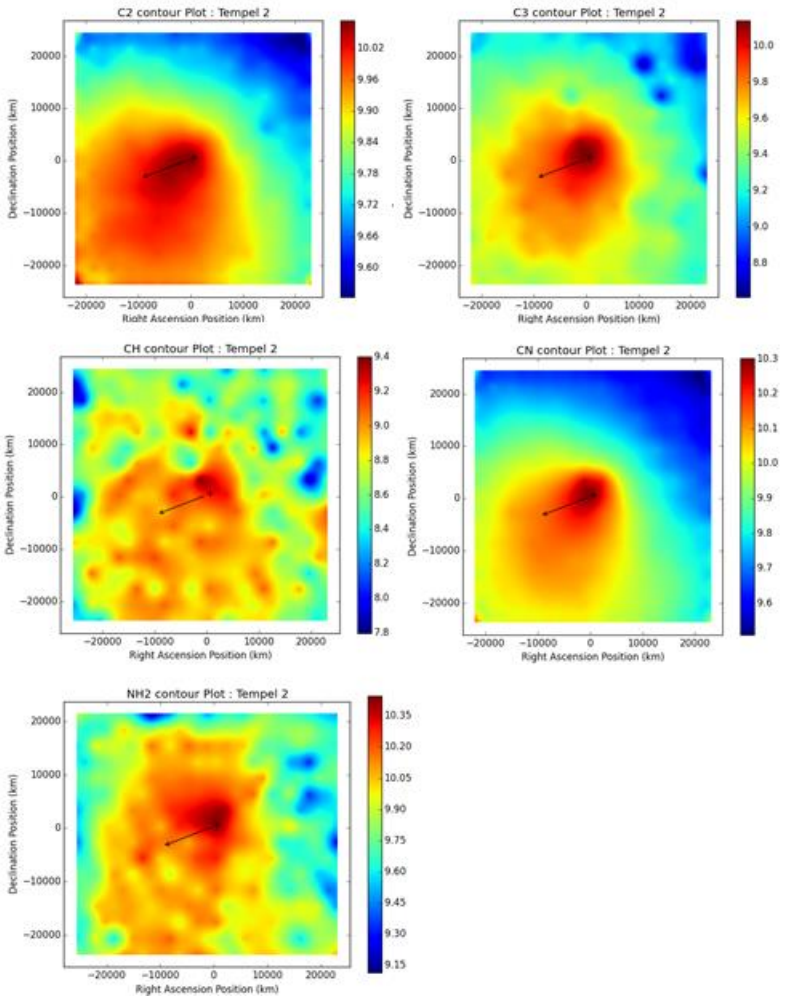

Figure 1 Contour plot of a sample IFU images

Figure 1 shows contour plots of a sample IFU image from a Tempel 2 observation for each species. The outwards vector indicates the direction of the Sun. Linear 2-D interpolation is used between fibers.

The underlying goal of this work is to model the behavior of the path integral of the column density, as a function of the radial distance from the center of the nucleus, which decreases exponentially. Modeling this behavior is much easier if we can assume symmetry with respect to position angle in the image. To facilitate this, instead of using all 247 fiber measurements, we construct an azimuthal average profile. Constructing the azimuthal average profile involves averaging fiber values along concentric rings about

the opto-center. In traditional narrowband photometry, the rings are chosen arbitrarily because traditional imaging data are spatially continuous. In our case, we are dealing with discrete values for column density with distance from the opto-center. Fortunately, the spatial distribution (gaps between) of the fibers in the IFU are hexagonally symmetric as seen in Figure 2. Due to this symmetry, we can form rings of fibers (usually in pairs of 6 or 12 fibers) which are all equal distance from the opto-center, with the one caveat that we are limited in how many rings we can form. This caveat can be problematic if the comet is off-center or we have too many missing fiber values, and causes some of the observations to be not included in the analysis of this work.

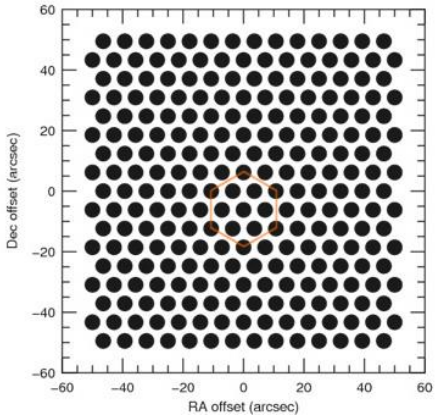

Figure 2 Spatial distribution of fibers of fibers for the IFU spectrograph

Datasets Included in the Study

The following observations were made for this study:

- One single observation of C_2, C_3, and CN was obtain for comet Faye on November 22, 2006.

- Four consecutive observations of all five species were obtained for comet Tempel 2 on July 15, 2010; however, only the first three produced a clean azimuthal average profile that could be used in the analysis.
- Five consecutive observations of all five species were obtained for comet Tempel 2 on September 13, 2010. The last observation was noticeably noisier than the previous four but was still included in the study.
- 13 consecutive observations of all fives species were obtained for comet Garradd on August 21, 2011; however, one was so off-center that concentric rings could not be formed around the opto-center and was excluded from the study.
- 9 consecutive observations of all five species were obtained for comet Garraad on Aug 22, 2011; however, only 6 were centered enough to construct an azimuthal average profile.

Observation Parameters

Table 1 Observation Dates and Heliocentric and Geocentric Distances

Comet	Observation Date	r_H (AU)	Δ (AU)
4P/Faye	2006 Nov 22	1.67	0.74
10P/Tempel 2	2010 Jul 15	1.43	0.72
10P/ Tempel 2	2010 Sept 13	1.60	0.67
C/2009 P1 Garradd	2011 Aug 21-22	2.27	1.39

Table 2 Observation Time for Faye

Label	Start time (UT)	Duration (s)
1	02:03	300

Table 3 Observation Times for Tempel 2

Label	Start time (UT)	Duration (s)
July 15:		
278	08:39	300
279	08:48	600
280	09:03	900
Sept 13:		
400	09:08	600
401	09:22	900
402	09:39	900
407	11:08	900
408	11:25	600

Table 4 Observation Times for Garradd

Label	Start time (UT)	Duration (s)
Aug 21:		
944	2:45	600
946	3:19	600
948	3:46	600
950	4:17	600
952	4:47	600
958	6:19	600
960	6:50	600
962	7:51	600
964	7:53	600
966	8:26	600
968	8:59	600
Aug 22:		
35	4:47	600
39	5:53	600
42	6:35	600
46	7:39	600
51	9:01	600
54	9:39	600

CHAPTER III

METHODS

The Haser model (Haser 1957) uses a given parent and daughter scale length (the lifetime, L, (in s) of the radical species times the outflow velocity, v, (in km/s) and is denoted S), production rate (in molecules/s), and heliocentric distance (in AU) to produce a radial profile (column density as a function of distance from the nucleus). It assumes the nucleus is spherical, uniformly outgassing, and that the parent and daughter velocities are purely radial. The model assumes a radial density distribution of

$$n_p(r) = \frac{Q_p}{4\pi r^2 v_p} e^{-\frac{r}{S_p}} \quad (1)$$

where $n_p(r)$ is the number density (in molecules/km^3) of the parent molecules as a function of r (in km) the distance from the nucleus. Q_p is the production rate of the parent molecule, and v_p is the velocity of the parent molecule (in km/s). A two stage approach where the parent molecule photo-dissociates into the daughter species yields

$$n_d(r) = \frac{Q_d}{4\pi r^2 v_d} \frac{S_d}{S_d - S_p} \left(e^{-\frac{r}{S_d}} - e^{-\frac{r}{S_p}} \right) , \quad (2)$$

where variables with the subscript d denote the daughter and those with subscript p denote the parent. This gives us the radial density profile of the daughter molecule (the one we observe). However, we observe the line-of-sight integral of the column density(M). If we assume the coma is optically thin (optical depth ≤ 1), we can derive an expression for M

$$M(\rho) = \frac{Q_d \rho}{v_d}\left(\int_x^{\mu x} K_0(y)dy + \frac{1}{x}\left(1 - \frac{1}{\mu}\right) + K_1(\mu x) + K_1(x)\right) \quad (3)$$

where ρ is a cylinder radius along the line of sight,x $= \frac{\rho}{S_d v_d}$, $\mu = \frac{S_p v_p}{S_d v_d}$, and $K_{0,1}$ are modified Bessel functions of the second kind and order 0 or 1 (Krishna Swamy 1986).

Haser Model Shape

- The vertical height or "y-intercept" of $n_d(r)$ vs r is dictated by Q_d .
- The slope of $n_d(r)$ vs r is affected by S_p and S_d and most dominantly by S_p/S_d.
- In Figure 3, the shape of $n_d(r)$ vs r is demonstrated for various values of S_p/S_d. For Figure 3, the following parameters were chosen arbitrarily to be $v_d = 0.85$ km/s , $Q_d = 5 \times 10^{24}$ molecules/s , and $S_d = 1.7 \times 10^5$km .

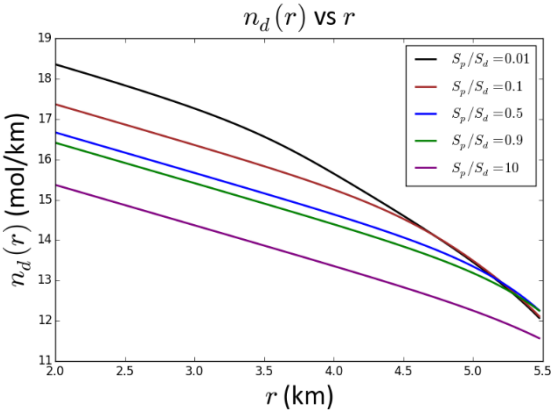

Figure 3 Haser model curves for various ratios of S_p/S_d

Fixed Parameters

Outflow velocity of the radical species is in the radial direction. The same outflow velocity is used for both daughter and parent species. The outflow velocity normalized to 1 AU used is $v(1\text{ AU}) = 0.85$ km/s , which is consistent with (Cochran 2012; Delsemme 1982). Other sources use 1 km/s (A'Hearn 1995). The heliocentric distances of the comet at the date of observation are listed in Table 1.

- The scale length is scaled by a power law using the heliocentric distance ($r_H{}^n$). For this work, $n = 2.0$ was chosen for all species, except for C_2 where $n = 2.5$ was chosen (Cochran 2012).
- Daughter Lifetimes (normalized to 1 AU) used are given in Table 5 below (Cochran 2012).

Table 5 Daughter Lifetimes

Species	Lifetime (s)
C_2	1.2e5
C_3	1.5e5
CH	4.8e3
CN	3.0e5
NH_2	6.2e4

Free Parameters

Production Rate

The production rate (Q_d) is the number of daughter molecules produced in the coma per second. For a given production rate and parent and daughter scale length, we compute R^2 (the coefficient of determination) between the radial profile produced by the

Haser model and the Azimuthal Average Profile. The coefficient of determination is defined to be 1 - (sum of residuals / sum of squares) . By constructing an array of production rates and running the Haser model for each one, we can find the global maximum of the R^2 vs Q_d curve. This allows us to determine the production rate for a given set of parent and daughter scale lengths.

Parent Lifetime

The purpose of this work is to determine the possible parent lifetime (L_p). We construct an array of L_p values, then run the Haser model for each value. For each L_p, we run through an array of Q_d values. Our result is a R^2 vs L_p curve which has a global maximum. The global maximum gives us the best fit L_p. For species C_2, CN, and NH_2 we use a 100 element array of L_p values between 1×10^2 s and 1×10^5 s (ie. [1×10^3, 2×10^3, …, 9.9×10^4, 1.0×10^5]. For C_3, we use values between 1×10^2 s and 1×10^4 s (ie. [1×10^2, 2×10^2, …, 9.9×10^3, 1.0×10^4]).

Optimization

The above mentioned method can be unnecessarily computational intensive, especially for observations with high flux values. To remedy this, instead of running through an array of Q_d values (converges in O(n)), we use the golden section search algorithm to find the optimal Q_d value for a given L_p (converges in O(log(n)). The expression O(f(n)) denotes big O notation, which quantifies the limiting behavior with function f. The golden section search algorithm is an iterative method which reduces the range of values the maximum or minimum is contained in with each iteration. The range

reduction at each iteration is proportional to the golden ratio and hence was named after the golden ratio (Kiefer 1953).

Model Fit Examples

Figures 4, 5, and 6 give some examples of Haser model fits to the azimuthal average profile. The red plus signs indicate the azimuthal average profile obtained from observations. The blue line indicates the Haser model fit.

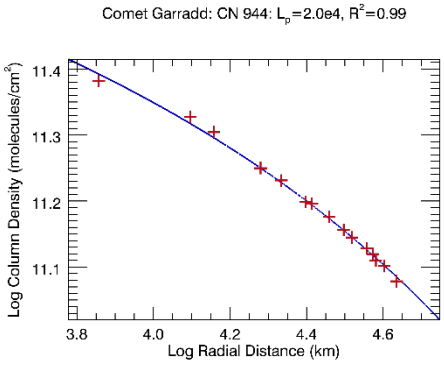

Figure 4 Example of a Haser model fit to the azimuthal average profile, where the L_p used gives the least-squares fit

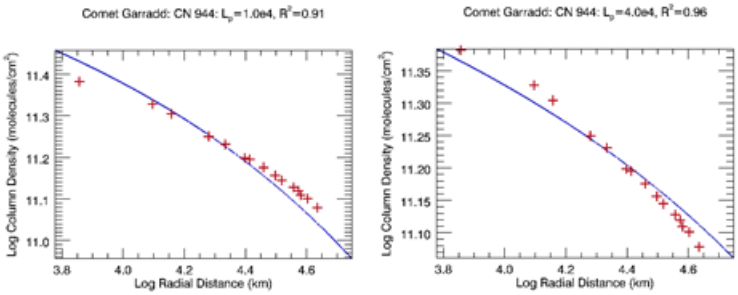

Figure 5 Example where the L_p used is half (on the left) and double (on the right) of the least-squares fit value

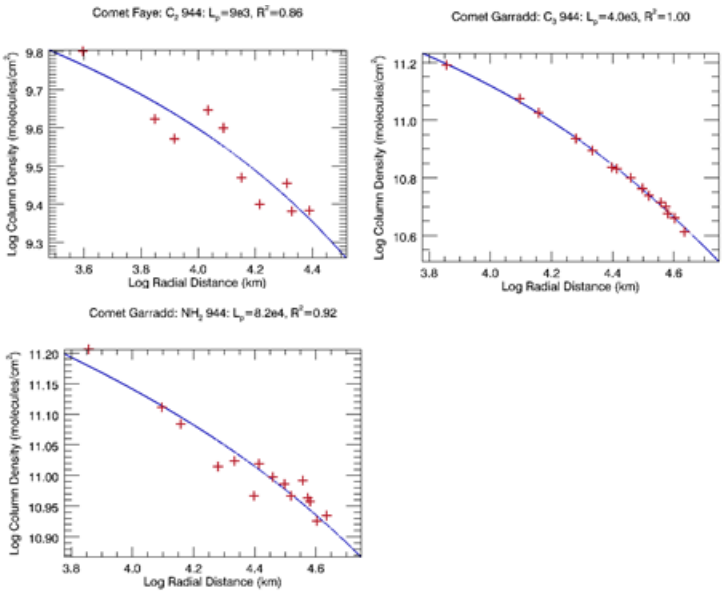

Figure 6 Examples of least-squares fit for L_p for all of the species observed

Note: CH and CN are exclude because they are already shown in Figures 4 and 5.

CHAPTER IV

RESULTS

Comet 4P/Faye

In Figure 7 below, curves of R^2 vs L_p are given for each observed species. The vertical line represents the parent lifetime for the particular species cited in Cochran 2012. The peak of each curve in Figure 7 above represents the best fit L_p. While CN provides a fairly clean result, both C_2 and C_3 suffer from fitting issues due to a noisy azimuthal average profile.

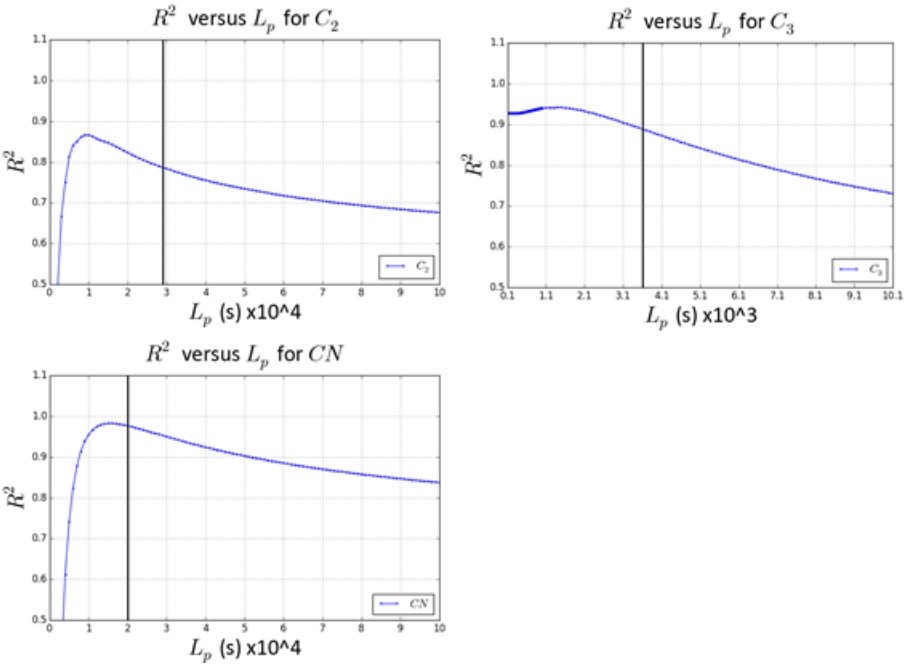

Figure 7 R^2 vs L_p curves for Faye

Table 6 Best Fit L_p for Each Species for Faye

Observation	L_p (s)	R^2
C_2	9E+03	0.87
C_3	1.40E+03	0.94
CN	1.6E+04	0.98

Table 7 compares our results to other cited L_p values by looking at where those lifetimes fall on our R^2 vs L_p curves. The R^2 values in Table 7 represent the fit error corresponding to using the cited L_p value for a Haser model fit.

Table 7 Comparison of Best-Fit Results for Faye to Other Results

Daughter Species	Parent Species	L_p (s)	R^2	Source
CN	N/A	2.0E+04	0.98	Cochran 1985
	N/A	3.5E+04	0.94	Festou et al. 1998
	N/A	2.4E+04	0.97	Feldman 2004
	N/A	1.3E+04	0.98	Randall et al. 1993
	HCN	9.1E+04	0.85	Jackson 1976 *
	HCN	7.7E+04	0.86	Huebner and Carpenter 1979, Huebner1985, Huebner et al. 1992
	HCN	6.7E+04	0.87	Bockeleé-Morvan and Crovisier 1985
	HCN	2.2E+06		Fray et al. 2005
	HC_3N	1.3E+04	0.98	Jackson 1976 *
	HC_3N	3.6E+04	0.93	Huebner and Carpenter 1979, Huebner 1985
	HC_3N	2.6E+04	0.96	Huebner et al. 1992
	HC_3N	2.9E+04	0.95	Krasnopolsky 1991
	HC_3N	1.5E+04	0.98	Crovisier 1994
	CH_3CN	1.5E+05		Bockeleé-Morvan and Crovisier 1985
	C_2N_2	1.1E+04	0.96	Jackson 1976 *
	C_2N_2	3.2E+04	0.94	Bockeleé-Morvan and Crovisier 1985
C_3	N/A	3.6E+03	0.89	Cochran 1985
	N/A	3.0E+03	0.91	Randall et al. 1992
	N/A	2.8E+03	0.91	Randall et al. 1993
	C_3H_2	7.7E+03	0.78	Helbert 2003
C_2	N/A	2.9E+04	0.79	Cochran et al. 1992
	C_2H_2	7.1E+04	0.70	Crovisier 1994

Note: * denotes results based on laboratory experiments, all other sources are from comet observations.

Comet 10P/Tempel 2

In Figure 8, curves of R^2 vs L_p are given. All of the datasets from the same observation date and species are graphed in the same window for comparison purposes. The vertical line represents the L_p value for the particular species cited in Cochran 2012. The syntax (400,401,…,etc.) label the observations. To see R^2 values on these R^2 vs L_p curves for cited L_p values see Table 9.

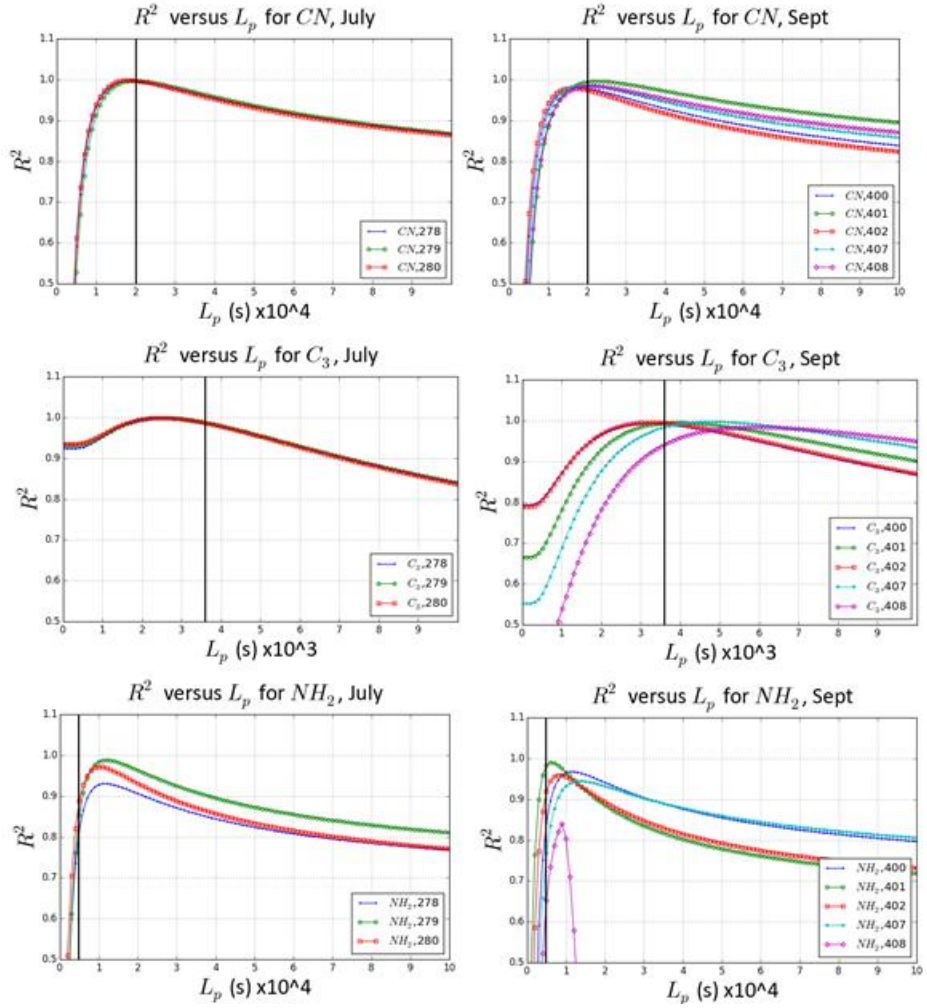

Figure 8 R^2 vs L_p curves for Tempel 2

The best fit L_p for each species and each observation date (averaged over all datasets) are given in Table 8. The best L_p value used for comparison to other works is the average of the July 15 and September 13 observations. Standard deviations (σ) are averaged for the best fit L_p. While there are many sources of error in the raw observations (ie. Instrument error, features in the coma, and the location of the opto-center), the primary source is photon shot noise. The resulting signal-to-noise ratio is not only an issue in this work, but in comet spectroscopy in general and often limits confidence levels in model results. The signal-to-noise ratio is likely higher near the opto-center where the intensity is the greatest and becomes lower in the outer coma. The July 15 observations provided a smaller set azimuthal rings (which cover a smaller radius) than the September 13 observations. This is a result of "pointing" issues with instrument at the time of the observations. Unfortunately, the signal-to-noise ratio for these observations are not well known as well as other sources of error; however, all uncertainties related to the raw observations manifest themselves in the final results of the analysis. Because we have multiple observations over a fairly short time interval, we can use the σ between best fit L_p values as our sole representation of measurement error.

Table 8 Best Fit L_p for Each Species for Tempel 2

Observation	L_p (s)	σ (s)
C_3 July	2.5E+03	1.0E+02
C_3 Sept	4.4E+03	1.4E+03
C_3 Avg	3.7E+03	1.4E+03
CN July	1.9E+04	1.0E+03
CN Sept	1.9E+04	2.7E+03
CN Avg	1.9E+04	2.1E+03
NH_2 July	1.1E+04	1.2E+03
NH_2 Sept	9.8E+03	3.2E+03
NH_2 Avg	1.0E+04	2.6E+03

The goal of this work is not only to determine L_p, but also to compare our L_p to previous work. Comparing to previous work is important because many of them are fairly discrepant from each other. Because we have standard deviations for each best fit L_p averaged over all observations, we can compare the L_p values cited in other works. We compare our results to other works be determining how many standard deviations away their results are from ours ($\Delta\sigma$). In Table 9, we catalog cited results from other works, and calculate $\Delta\sigma$ for the July 15, September 13, and overall. By looking at $\Delta\sigma$ for each work we can reasonable compare our results to theirs.

Table 9 Comparison of Best-Fit Results for Tempel 2 to Other Results

			Standard Deviations ($\Delta\sigma$)				
Daughter Species	**Parent Species**	L_p (s)	**July**	**Sept**	**Avg**	R^2	**Source**
CN	N/A	2.0E+04	1.0	0.2	0.4	0.96	Cochran 1985
	N/A	3.5E+04	16.0	5.8	7.4	0.99	Festou et al. 1998
	N/A	2.4E+04	4.5	1.5	2.0	0.99	Feldman 2004
	N/A	1.3E+04	6.0	2.4	2.9	0.97	Randall et al. 1993
	HCN	9.1E+04	71.9	26.5	33.8	0.87	Jackson 1976 *
	HCN	7.7E+04	57.9	21.3	27.2	0.89	Huebner and Carpenter 1979, Huebner 1985, Huebner et al. 1992
	HCN	6.7E+04	47.7	17.5	22.4	0.90	Bockeleé-Morvan and Crovisier 1985
	HCN	2.2E+06	2.20E+03	8.15E+02	1.04E+03		Fray et al. 2005
	HC_3N	1.3E+04	6.0	2.4	3.0	0.97	Jackson 1976
	HC_3N	3.6E+04	16.7	6.0	7.8	0.96	Huebner and Carpenter 1979, Huebner 1985
	HC_3N	2.6E+04	6.6	2.3	3.0	0.98	Huebner et al. 1992
	HC_3N	2.9E+04	10.4	3.7	4.8	0.97	Krasnopolsky 1991
	HC_3N	1.5E+04	3.8	1.6	1.9	0.98	Crovisier 1994
	CH_3CN	1.5E+05	1.30e2	48.1	61.3		Bockeleé-Morvan and Crovisier 1985
	C_2N_2	1.1E+04	8.0	3.1	3.9	0.94	Jackson 1976 *
	C_2N_2	3.2E+04	13.3	4.8	6.1	0.97	Bockeleé-Morvan and Crovisier 1985
C_3	N/A	3.6E+03	11.4	0.5	0.0	0.98	Cochran 1985
	N/A	3.0E+03	4.9	1.0	0.5	0.98	Randall et al. 1992
	N/A	2.8E+03	2.9	1.1	0.6	0.98	Randall et al. 1993
	C_3H_2	7.7E+03	51.8	2.3	2.8	0.91	Helbert 2003
NH_2	N/A	4.8E+03	5.6	1.6	2.1	0.84	Cochran et al. 1992
	N/A	4.0E+03	6.4	1.8	2.4	0.76	Krasnopolsky and Tkachuk 1991 / Fink et al. 1991
	NH_3	2.1E+04	8.2	3.5	4.0	0.83	Jackson 1976 *
	NH_3	5.6E+03	5.0	1.3	1.8	0.89	Huebner and Carpenter 1979, Huebner 1985, Huebner et al. 1992
	NH_3	6.7E+03	4.0	1.0	1.4	0.92	Allen 1987
	NH_3	5.6E+03	5.0	1.3	1.8	0.89	Hatchell et al. 2005

Note: * denotes results based on laboratory experiments, all other sources are from comet observations.

Comet C/2009 P1 Garradd

The same analysis that was done for Tempel 2 is performed for Garradd and is presented below. In Figures 9 and 10, we can see that for both CN and C_3, we see achieve a very high R^2 and very consistent results between observations. The NH_2 results are inconsistent; however, they all consistently disagree with the L_p value used in Cochran 2012 which is represented by the vertical line.

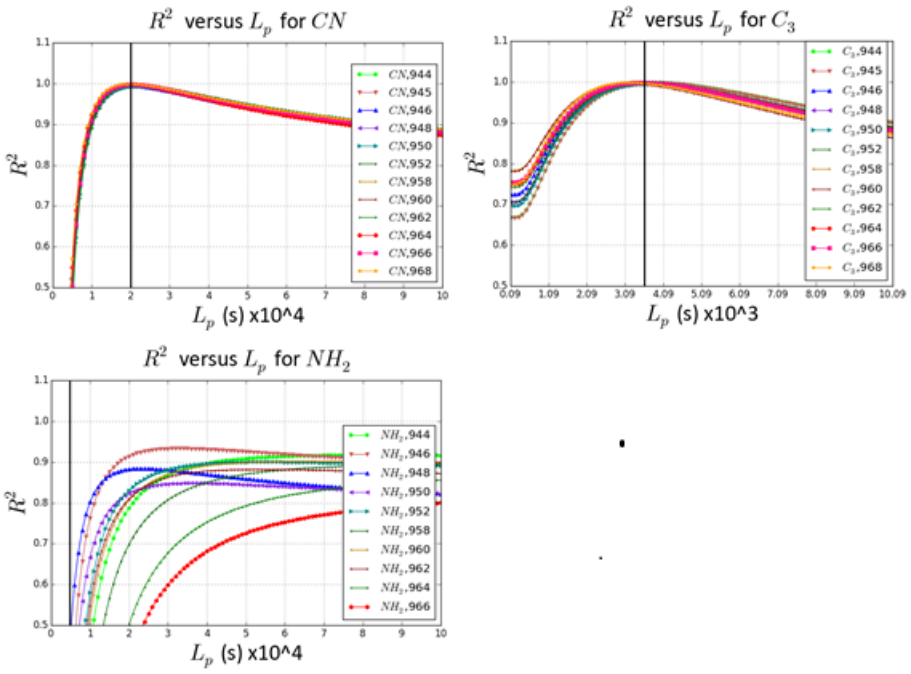

Figure 9 R^2 vs L_p for Garradd for Aug 21 Observations

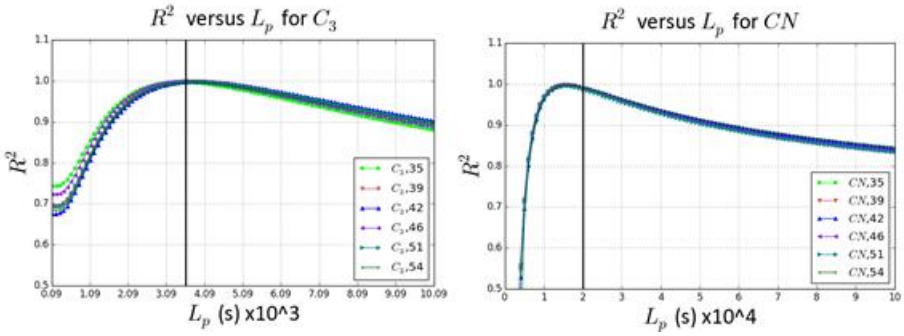

Figure 10 R^2 vs L_p for Garradd for Aug 22 Observations

Table 10 Best Fit L_p for Each Species for Garradd

Observation	L_p (s)	σ (s)
C_3 Aug 21	3.6E+03	2.3E+02
C_3 Aug 22	3.7E+03	1.5E+02
C_3 Avg	3.7E+03	2.2E+02
CN Aug 21	2.1E+04	9.1E+02
CN Aug 22	1.5E+04	5.2E+02
CN Avg	1.8E+04	2.6E+03
NH_2 Aug 21	5.0E+04	2.1E+04

Table 11 Comparison of Best-Fit Results for Garradd to Other Results

			Standard Deviations ($\Delta\sigma$)				
Daughter Species	**Parent Species**	L_p (s)	**21-Aug**	**22-Aug**	**Avg**	R^2	**Source**
CN	N/A	2.0E+04	0.6	9.0	0.8	0.99	Cochran 1985
	N/A	3.5E+04	16.0	38.1	6.5	0.96	Festou et al. 1998
	N/A	2.4E+04	3.3	15.9	2.1	0.99	Feldman 2004
	N/A	1.3E+04	8.3	4.5	1.9	0.98	Randall et al. 1993
	HCN	9.1E+04	77.8	146.4	27.9	0.87	Jackson 1976 *
	HCN	7.7E+04	62.4	119.3	22.5	0.88	Huebner and Carpenter 1979, Huebner 1985, Huebner et al. 1992
	HCN	6.7E+04	51.0	99.4	18.6	0.90	Bockeleé-Morvan and Crovisier 1985
	HCN	2.2E+06	2.4E+03	4.3E+03	8.4E+02		Fray et al. 2005
	HC_3N	1.3E+04	8.3	4.5	1.9	0.98	Jackson 1976 *
	HC_3N	3.6E+04	16.8	39.5	6.8	0.96	Huebner and Carpenter 1979, Huebner 1985
	HC_3N	2.6E+04	5.7	20.0	2.9	0.98	Huebner et al. 1992
	HC_3N	2.9E+04	9.9	27.3	4.4	0.97	Krasnopolsky 1991
	HC_3N	1.5E+04	5.9	0.4	1.1	0.99	Crovisier 1994
	CH_3CN	1.5E+05	142.3	259.3	50.1		Bockeleé-Morvan and Crovisier 1985
	C_2N_2	1.1E+04	10.5	8.4	2.6	0.96	Jackson 1976 *
	C_2N_2	3.2E+04	13.0	32.8	5.5	0.97	Bockeleé-Morvan and Crovisier 1985
C_3	N/A	3.6E+03	0.4	0.6	0.0	1.00	Cochran 1985
	N/A	3.0E+03	2.5	4.9	3.0	0.99	Randall et al. 1992
	N/A	2.8E+03	3.4	6.2	3.9	0.99	Randall et al. 1993
	C_3H_2	7.7E+03	18.2	26.3	18.7	0.94	Helbert 2003
NH_2	N/A	4.8E+03	2.2	N/A	N/A	0.14	Cochran et al. 1992
	N/A	4.0E+03	2.2	N/A	N/A	0.05	Krasnopolsky and Tkachuk 1991 / Fink et al. 1991
	NH_3	2.1E+04	1.4	N/A	N/A	0.84	Jackson 1976 *
	NH_3	5.6E+03	2.2	N/A	N/A	0.24	Huebner and Carpenter 1979, Huebner 1985, Huebner et al. 1992
	NH_3	6.7E+03	2.1	N/A	N/A	0.37	Allen 1987
	NH_3	5.6E+03	2.2	N/A	N/A	0.24	Hatchell et al. 2005

Note: * denotes results based on laboratory experiments, all other sources are from comet observations.

CHAPTER V

CONCLUSIONS AND FUTURE WORK

For the first time, comet data obtained from the Mitchell spectrograph is studied in depth using the Haser model in order to constrain possible parent lifetimes of radical species observed in cometary comae. By allowing both Q_d and L_p to be free parameters, we obtain results that not only indicate ideal parent candidates but also demonstrate error in the measurements and the limits of the Haser model.

Conclusions

Modeling C_2 proved unsuccessful. If we assumed the data was not noisy and that the Haser model isn't violating any assumptions, our results would conclude that the parent of C_2 has a very large lifetime. If we consider a lower limit of $R^2 = 0.95$, we get L_p values ranging between approximately 9e4 s and 6e5 s. Since R^2 vs L_p curves didn't yield peaks, we cannot demonstrate that the data were not noisy. Therefore, it would be unwise to make such a conclusion or any conclusion regarding C_2. Other works have also found significant issues with modeling C_2 distributions in cometary comae. In fact, there is a well-known discrepancy between C_2 distributions in the inner coma and in the outer coma (Feldman 2004). Due to our large field of view, our data are almost completely outer coma (with the exception of the one fiber centered at the optocenter).

CN provides the cleanest signal, and thus highlights the successes of this work and the robustness of the Haser model. Our results are consistent amongst all observations and comets presented in this work. We see excellent agreement with Cochran (1985); however, those results are from a large consortium of comet observations and do not assume a specific parent species. HCN is detected in comets and is a very plausible parent candidate. There is much debate as to whether HCN is a dominant or minor contributor to CN (Feldman). HCN does not seem to be a likely dominant parent for any comet observation in this study. Fray (2005) finds that it is unlikely that HCN is the sole candidate for comets inside 3 AU. All of our observations are made inside 3 AU. Our analyses indicate that cited L_p values for C_2N_2 and CH_3CN give reasonable results using the Haser model, leading us to suggest them as the possible dominant parent of CN. While there is no reason to think C_2N_2 doesn't exist in comets, it has yet to be detected in cometary atmospheres. Many have speculated that C_2N_2 could be a good parent candidate (Bonev and Komitov 2000, Bockeleé-Morvan and Crovisier 1985, Fray 2005). CH_3CN has been detected in comets; however, the corresponding L_p cited by Bockeleé-Morvan and Crovisier (1985) is not consistent with our results. The L_p for HC_3N given by Crovisier (1994) proves reasonably consistent with our results. According to Crovisier (1994), the primary photo destructive reaction is: $HC_3N + photon \rightarrow H + C_3N$, and concludes that "HC_3N cannot be directly a parent for the cometary CN radical".

NH_2 was observed for comets Tempel 2 and Garradd, but not for Faye. It is generally accepted that NH_3 is the parent of NH_2 and is therefore the only parent species considered in this study. Our work on NH_2 indicates a much shorter L_p than is indicated

in other works. The only source that indicates a L_p reasonably consistent with our work is that of Jackson (1976), which is the only source mentioned that is based on laboratory experiments (as opposed to comet observations). Despite the consistency of this result amongst almost of the observations, it should be noted that the noise in the NH_2 data is quite high and is manifested in the deviations between the observations.

For C_3, speculation on parentage has yielded little success. Parent molecules with the appropriate decay chain have not yet been detected. In our results, we again see excellent agreement with Cochran (1985). The only relevant lifetime from a specific parent species that could be found for this work is C_3H_2 in Helbert (2003) and is significantly larger than our best case L_p. It should be noted that near the peak of the R^2 vs L_p curves for all C_3 observations has a notably small gradient of descent; therefore, we cannot conclude that the L_p given in Helbert (2003) is incompatible with our observations.

While CH was observed for both comets Tempel 2 and Garradd, fluctuations between each value in the azimuthal average profile were extremely high. Due to these fluctuations, and the fact that CH has a very short lifetime (due its low oscillator strength), implementing the Haser model on any of the CH datasets proved to be unfeasible.

Future Work

This work took the approach of modeling radical species in cometary comae using the Haser Model with L_d and Q_d as free parameters. Some thought was put into extending the list of free parameters.

The first possible additional free parameter that was considered was L_d. The values for L_d are fairly well agreed upon; however, they can vary based on various observational parameters such as solar activity and R_h. As mentioned before, L_d is scaled by R_h to account for this. Future work could involve quantifying the effect that solar activity has on the lifetimes. This may be preferable to setting L_d as another free parameter.

The second possible additional free parameter that was considered was the grandparent lifetime in a multi-generational Haser Model to account for known two-step dissociation chains for the radical species observed, such as $C_2H_2 \rightarrow C_2H \rightarrow C_2$.

Finally, we decided against extending the list of free parameters for two primary reasons:

1. It would heavily increase algorithm complexity, requiring the model code to be parallelized and distributed across a cluster in order to finish in any reasonable amount of time. Multi-dimensional optimization routines could dramatically reduce the algorithm complexity; however, we would lose valuable information about the shape of the cost function (the function we are optimizing), which is important for determining statistical significance.
2. It potentially introduces the issues of Overfitting, where the model begins to describe random error instead of exclusively the underlying physical dynamics. This is particularly true for the multi-generational approach where there may be many local optimums in the cost function. With our current approach, the cost function is convex in both dimensions (L_d and Q_d), which means there are no local optimums to cope with.

Conclusively, future work with more free parameters could be considered, but at the peril of the aforementioned issues. These issues could likely be resolved or navigated around with enough thoughtful effort, but is beyond the scope of this work. This work instead chooses a more robust but more restricted approach to constraining photochemical parentage in comets. Other resources for future work modeling cometary coma include the use of CHON grains as gas sources and the use of the Vectorial model for asymmetric coma (Ihalawela 2009).

REFERENCES

A'Hearn, M. F., Millis, R. L., Schleicher, D. G., Osip, D. J., & Birch, P. V., 1995, "The Ensemble Properties of Comets: Results from Narrowband Photometry of 85 Comets, 1976-1992", Icarus, 118, 223.

A'Hearn, M. F., 2004, "Cometary Science: The Present and Future", Comets II, 2004, p.17-22.

Allen 1987. "Evidence for methane and ammonia in the coma of comet P/Halley", Astronomy and Astrophysics (ISSN 0004-6361), vol. 187, no. 1-2, Nov. 1987, p. 502-512. BMFT-SNSF-supported research.

Bonev B. and Komitov B. ,2000, "New two-variable fits for the scale lengths of CN and its parent molecule in cometary atmospheres: Application to the identification of the CN parent" Bull. Am. Astron. Soc., 32, 1072.

Bockeleé-Morvan, D ; Crovisier, J.,1985, "Possible parents for the cometary CN radical - Photochemistry and excitation conditions", Astronomy and Astrophysics (ISSN 0004-6361), vol. 151, no. 1, Oct. 1985, p. 90-100.

Cochran, A. L., 1985, "A re-evaluation of the Haser model scale lengths for comets", AJ, 90, 2609 - 2614.

Cochran et al. 1992. "The McDonald Observatory Faint Comet Survey - Gas production in 17 comets", Icarus (ISSN 0019-1035), vol. 98, no. 2, Aug. 1992, p. 151-162.

Cochran, A. L., Barker, E.S., Caballero, M.D., & Györgey-Ries, J. 2009. "Placing the Deep Impact mission into context: Two decades of observations of 9P/Tempel 1 from McDonald Observatory", Icarus, 199, 119-128.

Cochran, A. L., Barker, E. S., & Gray, C. L. 2012. "Thirty Years of Cometary Spectroscopy from McDonald Observatory", Icarus, 218, 144.

Crovisier, J. 1994. "Photodestruction Rates for Cometary Parent Molecules", JGR, 99, 3777.

Delsemme, A., 1982. Chemical Composition of Cometary Nuclei. In: Wilkening, L.L. (Ed.), Comets, University of Arizona Press, Tucson, AZ, pp. 85–130.

Feldman, P. D., Cochran, A. L., & Combi, M. R. 2004. “Spectroscopic Investigations of Fragment Species in the Coma”, in Comets II (M. C. Festou, H. U. Keller, & H. A.Weaver, eds.), pp. 425 – 447. University of Arizona Press, Tucson, Arizona.

Festou, M. C., Barale, O., Davidge, T., Stern, S. A., Tozzi, G. P., Womack, M., & Zucconi, J. M. 1998. “Tentative Identification of the Parent of CN Radicals in Comets: C2N2”, BAAS, 30, 1089.

Fink et al. 1991. “Comet P/Halley - Spatial distributions and scale lengths for C2, CN, NH2, and H2O”, Astrophysical Journal, Part 1 (ISSN 0004-637X), vol. 383, Dec. 10, 1991, p. 356-371.

Fray, N., Bénilan, Y., Cottin, H., Gazeau, M. C., & Crovisier, J. 2005. “The Origin of the CN Radical in Comets: A Review from Observations and Models”, P & SS, 53, 1243.

Haser L. (1957) Bull. Acad. R. de Belgique, Classe de Sci. 43(5), 740750.

Hatchell, J., Bird, M. K., van der Tak, F. F. S., & Sherwood, W. A. 2005. “Recent Searches for the Radio Lines of NH3 in Comets”, A & A, 439, 777.

Helbert, J. 2003. “Studying the Longterm Evolution of Gas Activity in the Coma of Comet C/1995 O1 (Hale-Bopp), with a Special Focus on the Chemistry of Carbon Bearing Molecules”, PhD Thesis. Free University, Berlin.

Hill, G. J., et al. 2008 “Design, Construction, and Performance of VIRUS-P: The Prototype of a Highly Replicated Integral-Field Spectrograph for HET”. Proc. SPIE, 7014, 257.

Huebner 1985. “The photochemistry of comets”, IN: The photochemistry of atmospheres: Earth, the other planets, and comets (A86-21076 08-88). Orlando, FL, Academic Press, Inc., 1985, p. 437-481.

Huebner, W. F., Carpenter, C. W.: 1979, Los Alamos informal report LA-8085-MS

Huebner, W. F., Keady, J. J., & Lyon, S. P. 1992. “Solar Photorates for Planetary Atmospheres and Atmospheric Pollutants”, A & SS, 195, 1.

Ihalawela, Chandrasiri, 2009, “The Spatial Distribution of CN Radicals in The Coma of Comet Encke”, Master’s Thesis, Mississippi State University

Jackson, W. M. 1976. “The Photochemical Formation of Cometary Radicals”, J. Photochem. 5,107.

Kiefer, J. (1953), "Sequential minimax search for a maximum", Proceedings of the American Mathematical Society 4 (3): 502–506, doi:10.2307/2032161,JSTOR 2032161, MR 0055639

Krasnopolsky, V. A ; Tkachuk, A. Yu. “TKS-Vega experiment - NH and NH2 bands in Comet Halley”, Astronomical Journal (ISSN 0004-6256), vol. 101, May 1991, p. 1915-1919.

Randall et al. 1992. “Observational Constraints on Molecular Scalelengths and Lifetimes in Comets”, American Astronomical Society, 24th DPS Meeting, id.31.15-P; Bulletin of the American Astronomical Society, Vol. 24, p.1002

Randall et al. 1993. “Long-Slit Spectral Imaging of Comets Austin and P/Brorsen-Metcalf”, Lunar and Planetary Institute, 1993, p.251

Woodney, Laura M., 2000, “Chemistry in Comets Hale-Bopp and Hyakutake”, Ph.D. Thesis, University of Maryland